# Signatures of the Unruh Effect via High-Power, Short-Pulse Lasers ◇

C. Lang, P.G. Thirolf, D. Habs, A. Henig, D. Jung, D. Kiefer, J. Schreiber [a], and R. Schützhold [b]
[a] Imperial College, London/UK [b] Univ. Duisburg-Essen

The development of high-intensity, short pulse lasers opens up experimental access to ultra high field physics studies. This may grant access to the long-predicted Unruh effect, where an accelerated observer experiences the quantum vacuum as a thermal bath of particles with the Unruh temperature $kT_U = \hbar a/2\pi c$ [1]. The Unruh radiation is an analogon of thermal Hawking radiation of a Black Hole [2].

The most promising experimental approach to study the Unruh effect in the laboratory was proposed in 1999 by Chen and Tajima [3]. They suggested to use the interaction of a high intensity laser field with strongly accelerated electrons.

Nowadays high-intensity, short pulse lasers with powers exceeding 100 TW offer the unique opportunity to address this fascinating and fundamental field of physics in realistic experiments. Laser-accelerated electrons can be used as accelerated scatterers, generating real photons via non-inertial scattering of virtual photons from quantum vacuum fluctuations. Two different experimental scenarios can be envisaged. In scenario 1 the electrons will be laser-accelerated to relativistic energies (< GeV) within distances of only a few milimeters together with coherent harmonic focusing of a laser beam serving as an optical undulator. In scenario 2 the optical undulator will be replaced by a brilliant X-ray beam, while the electron bunch energy can be limited to e.g. 1 MeV.

Table 1 compiles the relevant parameters of the two experimetal scenarios. Our experimental approach favours the scenario 2 with low-energy laser accelerated electrons interacting with a brilliant X-ray beam used as an undulator due to a significantly improved ratio of the probability for Unruh photons emission with respect to the dominant background given by photons from linearly accelerated electrons (= classical Larmor radiation).

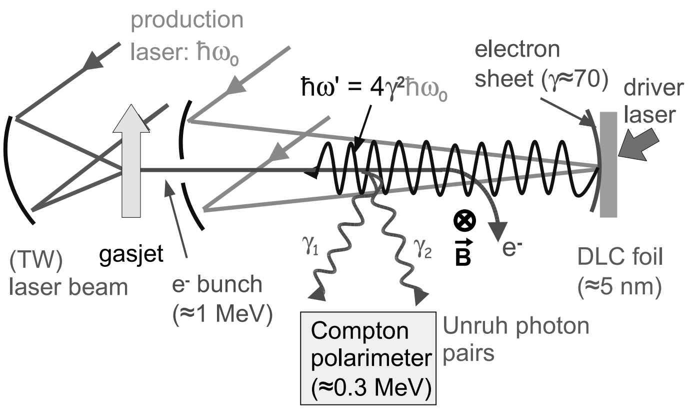


Fig. 1: Schematical view of an experimental setup for the detection of Unruh radiation originating from laser-accelerated electrons interacting with the strong periodic field of a counter-propagating X-ray beam.

Fig. 1 illustrates a possible experimental setup designed for the detection of Unruh photons generated in an experiment with oscillating electron acceleration [4]. Using a TW laser beam, electrons can be accelerated in a gas jet via the down-ramping technique [5] to monoenergetic energies around 1 MeV ($\gamma = 2$) with ca. $10^{10}$ electrons/bunch. These electrons are then injected into a counter propagating brilliant X-ray beam ($\approx 20$ keV) acting as an undulator. The X-rays will be produced via Compton backscattering of optical photons off a dense electron sheet, acting as a relativistic mirror [6]., In the oscillating field of the X-ray undulator entangled photon pairs will be generated as signatures of the Unruh effect (therefore called "Unruh photons"). The probability for Larmor photons will result in $P_{\mathrm{Larmor}} = 10^{-1}$, while the emission probability for Unruh photons amounts to $P_{\mathrm{Unruh}} = 10^{-6}$. This Unruh-to-Larmor-ratio (signal/background) can be improved to about $4 \cdot 10^{-3}$ by using a coincidence technique for photon pair detection [7]. About $10^3$ Unruh photons per second are expected.

Experimentally the generation of entangled Unruh photon pairs can be identified via Compton polarimetry, where a measurement of the azimuthal Compton scattering angle will be sensitive to the polarization of the detected photons (according to the Klein-Nishina formula).

For this purpose an advanced 2D-segmented position-sensitive planar germanium detector system was built by the company SEMIKON GmbH [8] (thickness 15 mm, 64x64 strips on each side, pitch size 1 mm). A photograph of the structured and contacted germanium crystal is shown in Fig. 2.

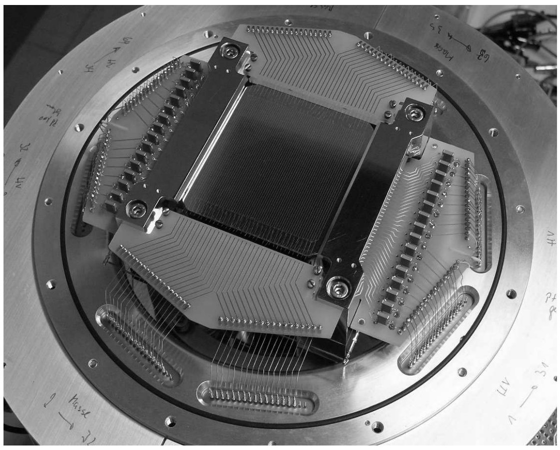

Fig. 2: 2D-segmented planar germanium Compton polarimeter, optimized for the detection of photons from Unruh (and Larmor) radiation with $E_\gamma < 300$ keV.

All strips have been tested by the manufacturer. An energy spectrum of a reference strip in the center of the crystal was measured (Fig. 3) with a shaping time of 0.5 $\mu$s and 2100 V bias voltage. The electronic noise level of all the strips on the high voltage side is shown in Fig. 4.

◇ Supported by the DFG Cluster of Excellence MAP (Munich-Centre for Advanced Photonics)

Related to the FWHM of the 60 keV line of the reference strip, the resolution of most of the strips can be estimated to be < 3 keV , except a region of strips at the borders of the crystal, where a larger width was measured (which is subject of ongoing improvement studies). On the ground side the noise of almost all of the strips is determined to be < 2 keV. The optimum bias voltage is about 2100 V. By increasing the bias voltage the resolution of the border strips will improve, however at the cost of an increase for the center strips. An optimum resolution measurement of all the 128 strips has to be performed with optimized shaping time and noise shielding conditions.

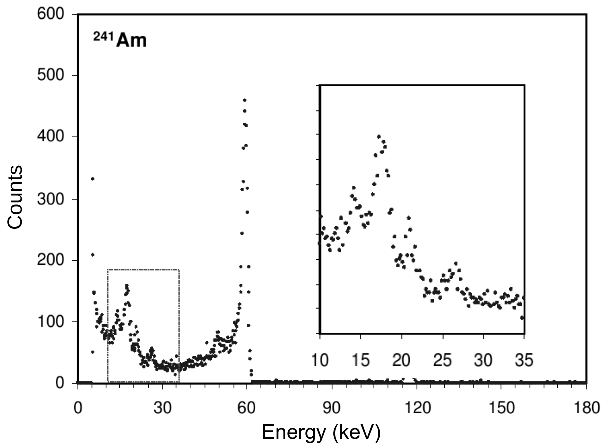


Fig. 3: Energy spectrum of a reference strip of the high voltage side in the center of the Ge crystal. Obtained from a $^{241}$Am source.

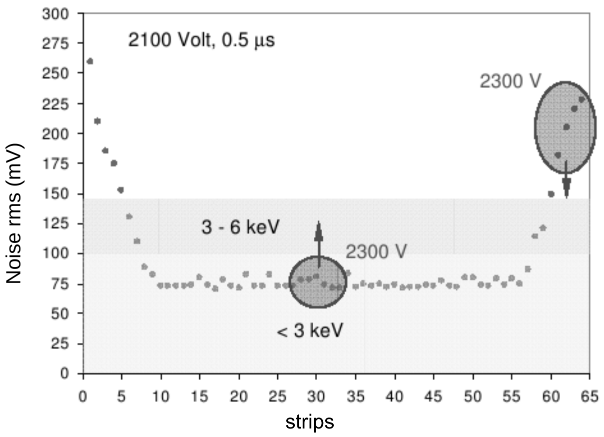


Fig. 4: Measured electronic noise level of all 64 strips on the high voltage side. The resolution is estimated by measuring the FWHM of a reference strip in the center region of the crystal.

In order to allow for a reliable operation of the detector system, an automatic LN2 filling system has been built. A schematical diagram of its layout is displayed in Fig. 5. The 150 liter dewar permanently operates at a pressure of < 3 bar. After a pre-defined time the magnetic valve no.1 opens to exhaust the pipe. When the thermal sensor PT1000 at the exhaust end detects liquid nitrogen, the magnetic valve no.1 closes and no.2 opens for filling the smaller dewar of the detector. The filling ends when the thermal sensor at the overflow detects liquid nitrogen. A USB module is continuously measuring the electric current through the PT1000 thermal sensors and calculating the temperatures. Its digital outputs open and close the magnetic valves. A warning system will report problems via e-mail and SMS.

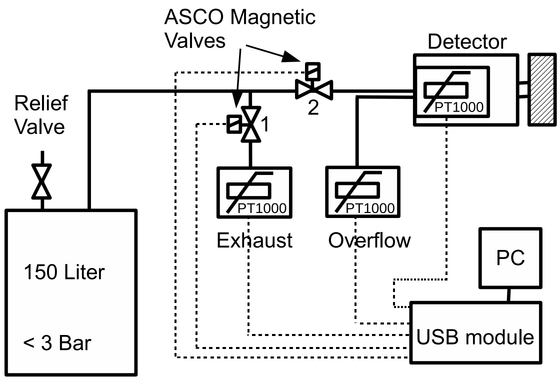


Fig. 5: Layout of the automatic LN2 filling system.

In the first phase it is envisaged to explore the experimental conditions for high-resolution $\gamma$ spectroscopy in the vicinity of high-intensity pulsed lasers interacting with matter in view of the resulting electromagnetic pulse.

Then the properties of the Larmor radiation will be studied, optimizing for coherent backscattering. Subsequently the search for signatures of the Unruh effect via the detection of entangled photon pairs will start, aiming at the first experimental identification of this fundamental process.

## References


[1] W.B. Unruh, Phys. Rev. D **14** (1976) 870
[2] S.W. Hawking, Comm. Math. Phys. **43** (1975) 194
[3] P. Chen and T. Tajima, Phys. Rev. Lett. **83** (1999) 256
[4] R. Schützhold, G. Schaller, D. Habs, Phys. Rev. Lett. **100** (2008) 091301
[5] C.G.R. Geddes *et al.* Phys. Rev. Lett. **100** (2008) 215004
[6] D. Habs *et al.* Appl. Phy. B **93** (2008) 349
[7] P.G. Thirolf *et al.* subm. to Eur. Phys. Journ. D
[8] SEMIKON Detector GmbH, www.semikon-detector.de


Table 1: Comparison of relevant parameters given for the two experimental scenarios discussed in the text for the creation of Unruh photon pairs with a summed energy of 900 keV (320 keV) for the scenario listed in the top (bottom) row.

| $N_\gamma$ /bunch | $E_{\mathrm{kin,e}}$ [MeV] | $\gamma$ | $I^{lab}$ [W/cm$^2$] | $I^{int}$ [W/cm$^2$] | $\hbar\omega_0$ (*:$\hbar\omega'$) [eV] | $\hbar\omega_{int}$ [eV] | $E^{lab}$ [V/m] | $E^{int}$ [V/m] | a [g] | $kT_U$ [eV] |
|---|---|---|---|---|---|---|---|---|---|---|
| $2\cdot 10^{15}$ | 150 | 300 | $10^{18}$ | $3.6\cdot10^{23}$ | 2.5 | $1.5\cdot10^3$ | $1.9\cdot 10^{12}$ | $1.2\cdot 10^{15}$ | $2.1\cdot10^{25}$ | 80 |
| $10^{13}$ | 1 | 2 | $2\cdot10^{25}$ | $3.2\cdot10^{26}$ | $2\cdot10^4$ * | $8\cdot10^4$ | $8.7\cdot 10^{15}$ | $3.5\cdot 10^{16}$ | $6.2\cdot10^{26}$ | $2.2\cdot10^3$ |